Nanoscale

COMMUNICATION

View Article Online
View Journal | View Issue

Cite this: *Nanoscale*, 2022, **14**, 299

Received 15th October 2021,
Accepted 29th November 2021

DOI: 10.1039/d1nr06821k

rsc.li/nanoscale

Templated synthesis enhances the cobalt adsorption capacity of a porous organic polymer†

Devin S. Rollins,[a] Charles P. Easterling,[b] Andrea N. Zeppuhar,[c] Jacob A. Krawchuck,[b] Timothy A. Dreier,[b] John Watt,[d] Dale L. Huber[b] and Mercedes K. Taylor*[c]

Divalent transition metals such as Co(II) are important targets for removal from water sources, due to their potential toxicity as well as their high value. In this study, we found that a series of porous organic polymers based on amide-linked tetraphenylmethane units are effective Co(II) ion adsorbents in aqueous solution. To increase the density of Co(II) binding sites, we then developed a templated synthesis in which the branched, rigid monomers are pre-assembled around Co(II) ions prior to polymerization. After polymer formation, the Co(II) template ions are removed to yield a material rich in Co(II) binding sites. Ion adsorption isotherms show that the Co(II)-templated material has an ion adsorption capacity significantly greater than those of the non-templated materials, highlighting the utility of a templated synthetic route. SEM and TEM images show the morphology of the templated polymer to be dramatically different from the non-templated polymers and to be similar in size and shape to the Co(II)–monomer precursors, emphasizing the role of the template ions in directing the formation of the resulting polymer. This guest-templated approach requires no functionalization of the generic monomer and represents a promising synthetic route to high-capacity ion adsorbents for water purification and aqueous separations.

Global fresh water supplies are increasingly stressed by population growth, industrialization, and climate change, trends that are likely to intensify in coming decades.[1–5] To address coming shortages in fresh water, there is a pressing need for technologies to purify alternative water sources such as wastewater or seawater.[6–9] Furthermore, these alternative water sources often contain valuable species (*e.g.*, precious metals and rare earth elements) that are desirable to capture *via* adsorption.[10,11] The design of high-performance adsorbents to remove trace toxic contaminants or precious elements from complex aqueous mixtures is consequently a priority in materials synthesis. Such adsorbents should feature a high density of binding sites for the adsorbate of interest while maintaining sufficient porosity to allow the adsorbate to diffuse into the interior of the material and access all binding sites, properties that can be synthetically difficult to install simultaneously.

Porous aromatic frameworks and other porous organic polymers have seen recent success in the area of aqueous ion adsorption. These materials are composed of branched, rigid building blocks that endow the polymer structure with permanent porosity, linked by covalent bonds that impart the necessary chemical stability for aqueous separations.[12–14] Porous organic polymers have shown promise in the capture of species such as $B(OH)_3$,[15] Cu^{2+},[16] Fe^{3+},[17] Nd^{3+},[18] $AuCl_4^-$,[19] Hg^{2+},[20] Pb^{2+},[21,22] and UO_2^{2+} (ref. 23 and 24) from aqueous solution. But laborious rounds of synthesis and functionalization are often necessary to discover the functionality and pore structure that maximize a material's adsorption capacity for a given adsorbate. A templated synthetic approach, where monomers are pre-assembled by the target adsorbate and then polymerized, can provide a short-cut to highly functional adsorbents. This approach has been widely studied for densely crosslinked non-porous polymers, but the resulting materials are plagued by low adsorption capacity because target adsorbates cannot penetrate the dense polymer matrix to access internal binding sites.[25,26] Porous organic polymers, on the other hand, are an exciting platform for the development of guest-templated adsorbents.[27–32] We hypothesized that by using branched, rigid monomers and selecting polymerization chemistry that would yield a rigid, water-stable linkage, a porous organic polymer could be templated by a generic adsorbate molecule to yield a high-capacity adsorbent.

[a]*Department of Chemistry, University of Washington, Seattle, WA 98195, USA*
[b]*Center for Integrated Nanotechnologies, Sandia National Laboratories, Albuquerque, NM 87123, USA*
[c]*Department of Chemistry and Biochemistry, University of Maryland, College Park, MD 20742, USA. E-mail: mkt@umd.edu*
[d]*Center for Integrated Nanotechnologies, Los Alamos National Laboratory, Los Alamos, NM 87545, USA*

†Electronic supplementary information (ESI) available: Syntheses, experimental procedures, and additional adsorption and materials characterization data. See DOI: 10.1039/d1nr06821k

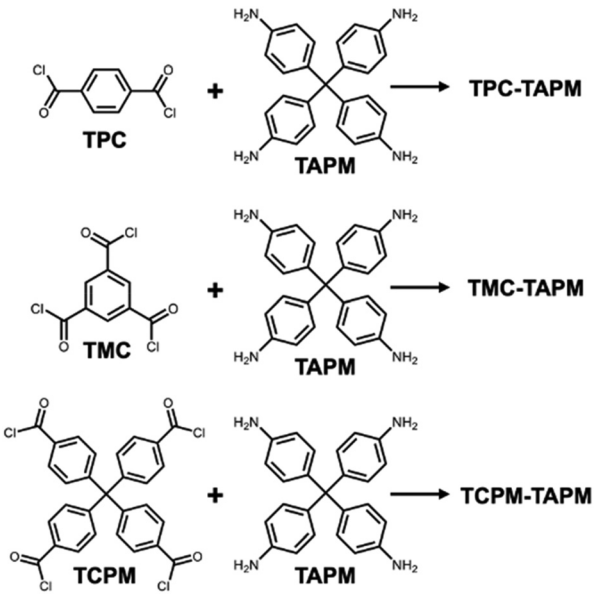

Scheme 1 Porous polyamides with increasing monomer branching.

To satisfy the criteria of branching and rigidity, we selected tetrakis(4-aminophenyl)methane (TAPM) as one of the two monomer partners in our route to porous organic polymers (Scheme 1). The amino groups on TAPM monomers were reacted with acyl chloride groups on a series of increasingly branched reaction partners (terephthaloyl chloride [TPC]; trimesoyl chloride [TMC]; tetraphenylmethane-4,4′,4″,4‴-tetraacyl chloride [TCPM]) to yield rigid and water-stable amide linkages throughout the resulting network. Polymerization conditions were adapted from the literature;[33,34] synthetic details are provided in the ESI.† The aromatic rings, amide linkages, and tetrahedral nodes present in the resulting polymers lead to a high degree of structural rigidity, which we hypothesized would preserve templated binding sites after the template was removed as well as provide significant internal porosity to allow ions to diffuse into the interior of the particles. In addition to the benefits of branching and rigidity, the long-term aqueous stability of amide bonds is well known as cross-linked polyamide materials are widely used in desalination membranes.[35]

The resulting non-templated polymers were termed TPC-TAPM, TMC-TAPM, and TCPM-TAPM (Scheme 1). Infrared spectroscopy and C/H/N analysis showed the formation of the desired amide-linked materials (see ESI†). The internal porosity of the three non-templated materials was assessed through N_2 adsorption isotherms (Fig. 1a). The BET surface areas of the three materials increase with increased monomer branching; the tetra-acyl chloride monomer (TCPM) endows the resultant polymer with the highest surface area (215 $m^2\ g^{-1}$), followed by the material based on the tri-acyl chloride monomer (TMC; 78 $m^2\ g^{-1}$) and then by the material based on the di-acyl chloride monomer (TPC; 31 $m^2\ g^{-1}$).

Among the large number of divalent metal ions that are important to capture from alternative water sources, Co(II) stands out as a useful probe molecule. In addition to being a

Mercedes K. Taylor

Dr Mercedes Taylor is an Assistant Professor in the Department of Chemistry and Biochemistry at the University of Maryland, College Park. She completed her PhD in chemistry at the University of California, Berkeley, where she studied gas adsorption in flexible metal–organic frameworks, and subsequently performed independent research at Sandia National Laboratories as a Jill Hruby Fellow. In 2021 she established her research lab at the University of Maryland, where her research group develops novel porous materials to better adsorb, separate and transport guest molecules in order to tackle problems in energy and sustainability.

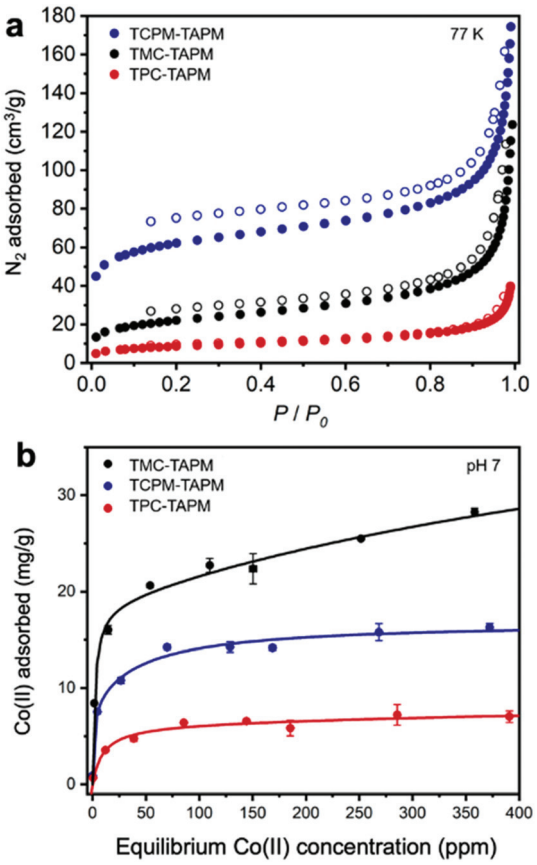

Fig. 1 N_2 adsorption isotherms at 77 K (a) and Co(II) adsorption isotherms in water at pH 7 (b) for TPC-TAPM (red), TMC-TAPM (black), and TCPM-TAPM (blue). For (a), solid circles represent adsorption and open circles represent desorption. For (b), circles represent ion adsorption data and solid lines represent dual-site Langmuir fits.

representative 2^+ transition metal cation, Co(II) is used in the manufacture of Li-ion batteries, and this application has resulted in skyrocketing demands for cobalt globally.[36] As a result of high demand and of cobalt's uneven distribution in the Earth's crust, cobalt mining has become associated with humanitarian, environmental, and geopolitical problems,[37] making the capture of Co(II) ions from water a priority.[38] Furthermore, Co(II) is toxic to both humans[39] and plants[40] at high levels, emphasizing the importance of Co(II) remediation from wastewater. Consequently Co(II) was selected as the template ion and target adsorbate in this study.

To test the Co(II) adsorption capacity of the non-templated control polymers TPC-TAPM, TMC-TAPM, and TCPM-TAPM, the polymers were individually submerged in water samples containing $CoCl_2$ at a range of concentrations (Fig. 1b). Cobalt concentrations before and after exposure to polymer samples were measured using inductively coupled plasma optical emission spectrometry (ICP-OES); detailed experimental procedures are provided in the ESI.† The results of the Co(II) adsorption experiments show all three porous polyamides to be effective ion adsorbents, adsorbing up to 28.3 mg Co per g polymer (TMC-TAPM) at the concentrations tested. Interestingly, the trend in ion adsorption capacity does not mirror the trend in N_2 adsorption capacity shown in Fig. 1a; while TCPM-TAPM has the highest N_2 adsorption capacity, TMC-TAPM is the leading Co(II) adsorbent. With ion capture from water as our ultimate priority, we selected TMC-TAPM as the platform for our templated synthesis.

To further increase the Co(II) capacity of TMC-TAPM, we modified the synthetic route to include a Co(II)-templating step (Fig. 2a). The modified synthesis begins by combining TAPM monomers with Co(II) ions, to form $Co_x(TAPM)_yCl_z$ complexes (Fig. 2a, Step 1). These complexes are then isolated and combined with a stoichiometric amount of the TMC monomer under standard polymerization conditions, leading to a polymerization reaction between TMC and the free amines from the $Co_x(TAPM)_yCl_z$ complexes (Fig. 2a, Step 2). Finally, an aqueous solution of dilute HCl is used to remove the bound Co(II) ions, leaving behind templated Co(II) binding sites in the final polymer (Fig. 2a, Step 3). Synthetic details are given in the ESI.†

Upon completion of Step 1, the $Co_x(TAPM)_yCl_z$ complexes were isolated as a pale purple solid. Scanning electron microscopy (SEM) revealed the complexes to be block-shaped crystallites approximately 20 μm in length (Fig. 2b). Powder X-ray diffraction (PXRD) data show the complexes to be crystal-

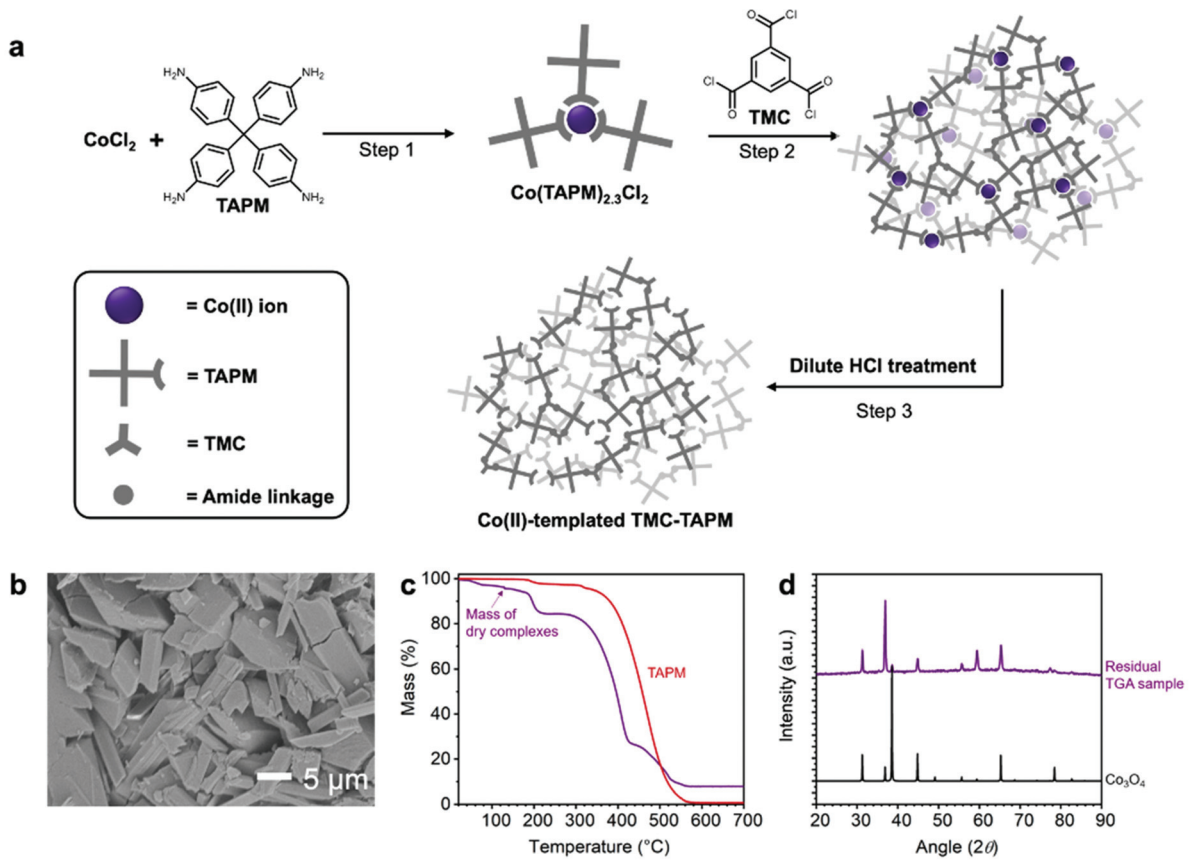

Fig. 2 (a) Schematic representation of the synthesis of Co(II)-templated TMC-TAPM. (b) Scanning electron microscope image of $Co(TAPM)_{2.3}Cl_2$ complexes. (c) Thermogravimetric analysis of $Co(TAPM)_{2.3}Cl_2$ complexes (purple) and TAPM (red). (d) Powder X-ray diffraction spectra of residual TGA sample (purple) and Co_3O_4 (black).

line and structurally distinct from the $CoCl_2$ and TAPM starting materials (Fig. S5†). To determine the exact composition of the $Co_x(TAPM)_yCl_z$ complexes, a sample was studied by thermogravimetric analysis (TGA), and the residue left over at the end of the TGA procedure was further analyzed by PXRD (Fig. 2c and d). By comparing the PXRD results to literature data,[41] the residual TGA sample was found to be Co_3O_4; this chemical formula was then used to calculate the mass of TAPM and chlorine that was lost during TGA, yielding a starting formula of $Co(TAPM)_{2.3}Cl_2$. The $Co(TAPM)_{2.3}Cl_2$ complexes were polymerized with a stoichiometric amount of TMC, followed by purification and activation to yield Co(II)-templated TMC-TAPM.

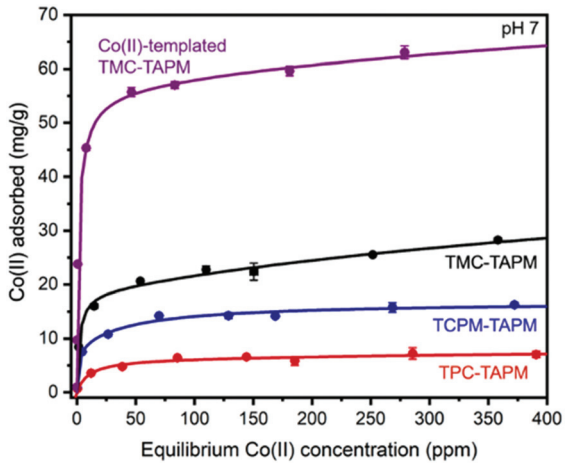

Fig. 3 Co(II) adsorption isotherms in water at pH 7 for Co(II)-templated TMC-TAPM (purple circles) as compared to those of TMC-TAPM (black circles), TCPM-TAPM (blue circles), and TPC-TAPM (red circles). The data were fit to multi-site Langmuir adsorption models (solid lines).

This material was then tested for Co(II) adsorption in an identical procedure to the non-templated materials, affording a Co(II) adsorption isotherm for the templated analogue (Fig. 3). In comparison to the non-templated control (TMC-TAPM), the templated analogue showed a dramatic improvement in Co(II) adsorption capacity. At the highest starting concentration tested (approx. 410 ppm Co), the Co(II)-templated material exhibits a Co(II) adsorption capacity more than twice as high as that of the non-templated control (63.0 mg g^{-1} *versus* 28.3 mg g^{-1}, respectively). The Co(II) adsorption results in Fig. 3 emphasize the advantages of a templating strategy when developing synthetic routes to novel ion adsorbents: the modified synthetic route shown in Fig. 2a installs significantly more Co(II) binding sites in the resulting polymer, compared to the non-templated synthesis, without necessitating arduous synthesis of custom monomers.

SEM images of the evacuated samples indicated a striking morphology difference between the templated and non-templated polymers (Fig. 4a). All of the non-templated materials (TPC-TAPM, TMC-TAPM, and TCPM-TAPM) display a rough surface morphology composed of agglomerated nanoscale particles, whereas Co(II)-templated TMC-TAPM is composed of intertwined stringy tendrils approximately 3 μm in diameter and approximately 20 μm in length. The similarity in size and shape of the Co(II)-templated TMC-TAPM particles in Fig. 4a to the $Co(TAPM)_{2.3}Cl_2$ complexes in Fig. 2b, along with their dissimilarity to the non-templated polymers in Fig. 4a, is clear evidence of the role played by Co(II) in directing the monomer arrangement during polymerization and driving the resulting polymer morphology. Transmission electron microscope (TEM) images show TPC-TAPM, TMC-TAPM, and TCPM-TAPM to be composed of agglomerated spheres with diameters of approximately 100 nm (Fig. 4b). These spherical agglomerates are also present in the TEM images of Co(II)-templated

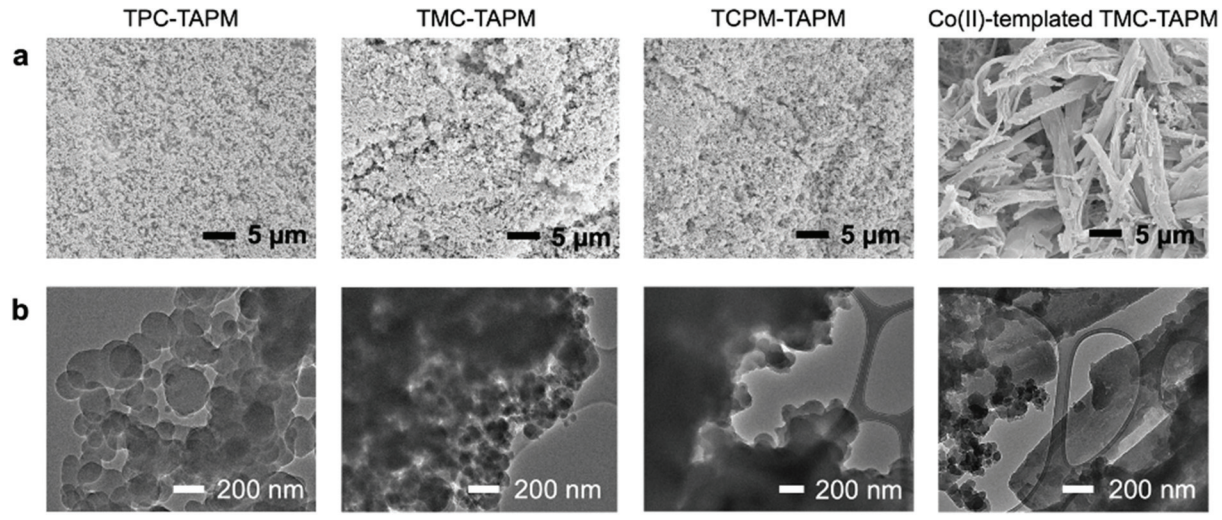

Fig. 4 (a) Scanning electron microscope images of activated TPC-TAPM, TMC-TAPM, TCPM-TAPM, and Co(II)-templated TMC-TAPM. (b) Transmission electron microscope images of TPC-TAPM, TMC-TAPM, TCPM-TAPM, and Co(II)-templated TMC-TAPM after exposure to aqueous solution containing 400 ppm Co(II) and subsequent drying to remove excess water.

TMC-TAPM, alongside the larger stringy tendrils, indicating the formation of some non-templated polymer along with the Co(II)-templated structures (Fig. 4b, right).

Co(II)-templated TMC-TAPM was found to have a BET surface area only 1/5th that of the non-templated TMC-TAPM (Fig. S10†), while still adsorbing twice as much Co(II). This divergence in adsorption trends for Co(II)-templated TMC-TAPM (high ion adsorption capacity; low N_2 adsorption capacity) echoes the divergent trends observed in Fig. 1a and b. These results may indicate that the N_2-accessible surface area measured on a dry powder under vacuum is not a particularly useful proxy for a material's porosity in aqueous solution. Water vapor adsorption isotherms may be a more useful measurement; vapor sorption experiments are planned for Co(II)-templated TMC-TAPM as a future direction. We also plan to test whether increasing the N_2-accessible surface area of a guest-templated material (by ball-milling the guest-monomer complexes before polymerization, for example) could further improve its guest adsorption capacity.

Additional ion adsorption experiments show Co(II)-templated TMC-TAPM to have a similarly high capacity for the transition metal ions Mn(II), Ni(II), and Zn(II) (Fig. S11†), making this material a promising adsorbent for a number of ions of interest. However, to separate complex mixtures of transition metals, even greater structural rigidity may be necessary in a templated polymer to insure selectivity among highly similar first-row divalent transition metal cations.

After aqueous Co(II) adsorption experiments, hydrated samples were flash frozen (vitrified) and analyzed by cryogenic scanning electron microscopy (cryo-SEM) and energy dispersive X-ray spectroscopy (EDX; Fig. S12–S15†). The EDX results show adsorbed Co distributed throughout the samples; in agreement with the aqueous adsorption data, EDX maps show a significant increase in Co density for Co(II)-templated TMC-TAPM relative to the non-templated polymers.

Conclusions

We have shown that a series of porous organic polymers, composed of highly branched monomers linked by amide bonds, are effective Co(II) adsorbents. Upon modifying the synthetic route to include a Co(II)-templating step, we found that the resultant Co(II)-templated polymer has a significantly improved Co(II) adsorption capacity (an increase of 2.2×) relative to the non-templated analogue TMC-TAPM. SEM and TEM images of the $Co(TAPM)_{2.3}Cl_2$ intermediate, the Co(II)-templated polymer, and the non-templated control polymers indicate that the $Co(TAPM)_{2.3}Cl_2$ intermediate greatly influences the resulting polymer morphology. N_2 adsorption isotherms of the series of polymers show a divergence between N_2-accessible porosity and aqueous ion adsorption capacity, indicating that water vapor adsorption isotherms may be a promising future direction to better characterize the structure of a porous organic polymer in aqueous solution. In summary, the guest-templated synthetic approach described herein is a promising and generalizable route to high-capacity, high-performance ion adsorbents.

Author contributions

Synthesis was carried out by D.S.R., C.P.E., and M.K.T. Gas sorption measurements were performed by M.K.T. Ion adsorption experiments were performed by D.S.R. and M.K.T. Materials characterization (TGA, PXRD, IR) was carried out by D.S.R. C.P.E., A.N.Z., T.A.D., and M.K.T. Electron microscopy (SEM, TEM, EDX) was carried out by J.A.K. and J.W. Project was formulated by D.L.H. and M.K.T. All authors contributed to manuscript preparation.

Conflicts of interest

There are no conflicts to declare.

Acknowledgements

We thank the University of Maryland College Park for funding. We gratefully acknowledge the support of the Center for Integrated Nanotechnologies, an Office of Science User Facility operated for the US DOE Office of Science. Sandia National Laboratories is a multimission laboratory managed and operated by National Technology and Engineering Solutions of Sandia, LLC, a wholly owned subsidiary of Honeywell International, Inc., for the US DOE's National Nuclear Security Administration (contract no. DE-NA-0003525). The views expressed in the article do not necessarily represent the views of the US DOE or the US government. Los Alamos National Laboratory, an affirmative action equal opportunity employer, is managed by Triad National Security, LLC for the U.S. Department of Energy's NNSA, under contract 89233218CNA000001. We are grateful to Todd Alam for performing solid-state NMR measurements and to Sergei Ivanov for helpful discussions.

References

1 M. M. Mekonnen and A. Y. Hoekstra, *Sci. Adv.*, 2016, **2**, e1500323.
2 M. A. Hanjra and M. E. Qureshi, *Food Policy*, 2010, **35**, 365.
3 C. J. Vorosmarty, P. Green, J. Salisbury and R. B. Lammers, *Science*, 2000, **289**, 284.
4 P. H. Gleick, *Science*, 2003, **302**, 1524.
5 A. Y. Hoekstra, M. M. Mekonnen, A. K. Chapagain, R. E. Mathews and B. D. Richter, *PLoS One*, 2012, **7**, e32688.
6 P. Gikas and A. N. Angelakis, *Desalination*, 2009, **248**, 1049.
7 M. Qadir, B. R. Sharma, A. Bruggeman, R. Choukr-Allah and F. Karajeh, *Agric. Water Manage.*, 2007, **87**, 2.
8 M. A. Shannon, P. W. Bohn, M. Elimelech, J. G. Georgiadis, B. J. Marinas and A. M. Mayes, *Nature*, 2008, **452**, 301.

9 G. M. von Medeazza, *Desalination*, 2004, **169**, 287.
10 D. S. Sholl and R. P. Lively, *Nature*, 2016, **532**, 435.
11 W. W. Li, H. Q. Yu and B. E. Rittmann, *Nature*, 2015, **528**, 29.
12 N. Chaoui, M. Trunk, R. Dawson, J. Schmidt and A. Thomas, *Chem. Soc. Rev.*, 2017, **46**, 3302.
13 S. Qiu and T. Ben, *Porous Polymers: Design, Synthesis and Applications*, Royal Society of Chemistry, Cambridge, UK, 2016.
14 Y. Tian and G. Zhu, *Chem. Rev.*, 2020, **120**, 8934.
15 J. Kamcev, M. K. Taylor, D.-M. Shin, N. N. Jarenwattananon, K. A. Colwell and J. R. Long, *Adv. Mater.*, 2019, **31**, e1808027.
16 S. Lee, G. Barin, C. M. Ackerman, A. Muchenditsi, J. Xu, J. A. Reimer, S. Lutsenko, J. R. Long and C. J. Chang, *J. Am. Chem. Soc.*, 2016, **138**, 7603.
17 S. Lee, A. Uliana, M. K. Taylor, K. Chakarawet, S. R. S. Bandaru, S. Gul, J. Xu, C. M. Ackerman, R. Chatterjee, H. Furukawa, J. A. Reimer, J. Yano, A. Gadgil, G. J. Long, F. Grandjean, J. R. Long and C. J. Chang, *Chem. Sci.*, 2019, **10**, 6651.
18 S. Demir, N. K. Brune, J. F. Van Humbeck, J. A. Mason, T. V. Plakhova, S. Wang, G. Tian, S. G. Minasian, T. Tyliszczak, T. Yaita, T. Kobayashi, S. N. Kalmykov, H. Shiwaku, D. K. Shuh and J. R. Long, *ACS Cent. Sci.*, 2016, **2**, 253.
19 T. Ma, R. Zhao, Z. Li, X. Jing, M. Faheem, J. Song, Y. Tian, X. Lv, Q. Shu and G. Zhu, *ACS Appl. Mater. Interfaces*, 2020, **12**, 30474.
20 B. Li, Y. Zhang, D. Ma, Z. Shi and S. Ma, *Nat. Commun.*, 2014, **5**, 5537.
21 Y. Yang, Z. Yan, L. Wang, Q. Meng, Y. Yuan and G. Zhu, *J. Mater. Chem. A*, 2018, **6**, 5202.
22 M. X. Tan, Y. N. Sum, J. Y. Ying and Y. Zhang, *Energy Environ. Sci.*, 2013, **11**, 3254.
23 Y. Yuan, Y. Yang, X. Ma, Q. Meng, L. Wang, S. Zhao and G. Zhu, *Adv. Mater.*, 2018, **30**, e1706507.
24 B. Li, Q. Sun, Y. Zhang, C. W. Abney, B. Aguila, W. Lin and S. Ma, *ACS Appl. Mater. Interfaces*, 2017, **9**, 12511.
25 C. Branger, W. Meouche and A. Margaillan, *React. Funct. Polym.*, 2013, **73**, 859.
26 J. Fu, L. Chen, J. Li and Z. Zhang, *J. Mater. Chem. A*, 2015, **3**, 13598.
27 Y. Yuan, Y. Yang and G. Zhu, *ACS Cent. Sci.*, 2020, **6**, 1082.
28 Y. Yuan, Y. Yang, M. Faheem, X. Zou, X. Ma, Z. Wang, Q. Meng, L. Wang, S. Zhao and G. Zhu, *Adv. Mater.*, 2018, **30**, 1800069.
29 H.-P. Hentze and M. Antonietti, *Curr. Opin. Solid State Mater. Sci.*, 2001, **5**, 343.
30 Q. Wei and S. L. James, *Chem. Commun.*, 2005, **12**, 1555.
31 S. Chakraborty, Y. J. Colón, R. Q. Snurr and S. T. Nguyen, *Chem. Sci.*, 2015, **1**, 384.
32 S.-C. Qi, G.-X. Yu, D.-M. Xue, X. Liu, X.-Q. Liu and L.-B. Sun, *Chem. Eng. J.*, 2020, **385**, 123978.
33 Z. Liu, J. Ou, H. Wang, X. You and M. Ye, *ACS Appl. Mater. Interfaces*, 2016, **8**, 32060.
34 H. Qian, S. Li, J. Zheng and S. Zhang, *Langmuir*, 2012, **28**, 17803.
35 J. R. Werber, C. O. Osuji and M. Elimelech, *Nat. Rev. Mater.*, 2016, **1**, 1.
36 Lithium-ion batteries need to be greener and more ethical, *Nature*, 2021, **595**, 7.
37 N. Niarchos, *The Dark Side of Congo's Cobalt Rush*. The New Yorker, 2021.
38 A. LiVecchi, A. Copping, D. Jenne, A. Gorton, R. Preus, G. Gill, R. Robichaud, R. Green, S. Geerlofs, S. Gore, D. Hume, W. McShane, C. Schmaus and H. Spence, *Powering the Blue Economy: Exploring Opportunities for Marine Renewable Energy in Maritime Markets*, U.S. Department of Energy, Office of Energy Efficiency and Renewable Energy, 2019.
39 L. Leyssens, B. Vinck, C. Van Der Straeten, F. Wuyts and L. Maes, *Toxicology*, 2017, **387**, 43.
40 P. C. Nagajyoti, K. D. Lee and T. V. M. Sreekanth, *Environ. Chem. Lett.*, 2010, **8**, 199.
41 I. N. Dubrovina and A. A. Shchepetkin, *Neorg. Mater.*, 1973, **9**, 474.

